

**UCC Library and UCC researchers have made this item openly available.  
Please [let us know](#) how this has helped you. Thanks!**

<b>Title</b>	Boosting biomethane yield and production rate with graphene: the potential of direct interspecies electron transfer in anaerobic digestion
<b>Author(s)</b>	Lin, Richen; Cheng, Jun; Zhang, Jiabei; Zhou, Junhu; Cen, Kefa; Murphy, Jerry D.
<b>Publication date</b>	2017-05-05
<b>Original citation</b>	Lin, R., Cheng, J., Zhang, J., Zhou, J., Cen, K. and Murphy, J. D. (2017) 'Boosting biomethane yield and production rate with graphene: The potential of direct interspecies electron transfer in anaerobic digestion', <i>Bioresource Technology</i> , 239, pp. 345-352. doi:10.1016/j.biortech.2017.05.017
<b>Type of publication</b>	Article (peer-reviewed)
<b>Link to publisher's version</b>	<a href="http://dx.doi.org/10.1016/j.biortech.2017.05.017">http://dx.doi.org/10.1016/j.biortech.2017.05.017</a> Access to the full text of the published version may require a subscription.
<b>Rights</b>	© 2017 Published by Elsevier Ltd. This manuscript version is made available under the <b>CC-BY-NC-ND 4.0 license</b> <a href="http://creativecommons.org/licenses/by-nc-nd/4.0/">http://creativecommons.org/licenses/by-nc-nd/4.0/</a>
<b>Embargo information</b>	Access to this article is restricted until 24 months after publication at the request of the publisher
<b>Embargo lift date</b>	2019-05-05
<b>Item downloaded from</b>	<a href="http://hdl.handle.net/10468/4060">http://hdl.handle.net/10468/4060</a>

Downloaded on 2021-11-27T04:49:09Z

## Accepted Manuscript

Boosting biomethane yield and production rate with graphene: the potential of direct interspecies electron transfer in anaerobic digestion

Richen Lin, Jun Cheng, Jiabei Zhang, Junhu Zhou, Kefa Cen, Jerry D. Murphy

PII: S0960-8524(17)30656-9  
DOI: <http://dx.doi.org/10.1016/j.biortech.2017.05.017>  
Reference: BITE 18043

To appear in: *Bioresource Technology*

Received Date: 13 March 2017  
Revised Date: 30 April 2017  
Accepted Date: 3 May 2017

Please cite this article as: Lin, R., Cheng, J., Zhang, J., Zhou, J., Cen, K., Murphy, J.D., Boosting biomethane yield and production rate with graphene: the potential of direct interspecies electron transfer in anaerobic digestion, *Bioresource Technology* (2017), doi: <http://dx.doi.org/10.1016/j.biortech.2017.05.017>

This is a PDF file of an unedited manuscript that has been accepted for publication. As a service to our customers we are providing this early version of the manuscript. The manuscript will undergo copyediting, typesetting, and review of the resulting proof before it is published in its final form. Please note that during the production process errors may be discovered which could affect the content, and all legal disclaimers that apply to the journal pertain.



1 **Boosting biomethane yield and production rate with graphene: the**  
2 **potential of direct interspecies electron transfer in anaerobic**  
3 **digestion**

4

5 **Richen Lin<sup>a,b,c</sup>, Jun Cheng<sup>a,\*</sup>, Jiabei Zhang<sup>a</sup>, Junhu Zhou<sup>a</sup>, Kefa Cen<sup>a</sup>, Jerry D. Murphy<sup>b,c</sup>**

6 <sup>a</sup> *State Key Laboratory of Clean Energy Utilization, Zhejiang University, Hangzhou 310027, China*

7 <sup>b</sup> *MaREI Centre, Environmental Research Institute, University College Cork, Cork, Ireland*

8 <sup>c</sup> *School of Engineering, University College Cork, Cork, Ireland*

9

10 **Abstract**

11 Interspecies electron transfer between bacteria and archaea plays a vital role in enhancing  
12 energy efficiency of anaerobic digestion (AD). Conductive carbon materials (i.e. graphene  
13 nanomaterial and activated charcoal) were assessed to enhance AD of ethanol (a key intermediate  
14 product after acidogenesis of algae). The addition of graphene (1.0 g/L) resulted in the highest  
15 biomethane yield ( $695.0 \pm 9.1$  mL/g) and production rate ( $95.7 \pm 7.6$  mL/g/d), corresponding to an  
16 enhancement of 25.0% in biomethane yield and 19.5% in production rate. The ethanol degradation  
17 constant was accordingly improved by 29.1% in the presence of graphene. Microbial analyses  
18 revealed that electrogenic species of *Geobacter* and *Pseudomonas* along with archaea  
19 *Methanobacterium* and *Methanospirillum* might participate in direct interspecies electron transfer  
20 (DIET). Theoretical calculations provided evidence that graphene-based DIET can sustained a  
21 much higher electron transfer flux than conventional hydrogen transfer.

---

\* Corresponding author: Prof. Dr. Jun Cheng, State Key Laboratory of Clean Energy Utilization, Zhejiang University, Hangzhou 310027, China. Tel.: +86 571 87952889; fax: +86 571 87951616. E-mail: juncheng@zju.edu.cn

1 **Keywords:** Graphene; activated charcoal; ethanol; direct interspecies electron transfer; anaerobic  
2 digestion.

3

## 4 **1. Introduction**

5 Anaerobic digestion (AD) of wet organic biomass for biogas production provides a  
6 sustainable route to reduce fossil fuel use and greenhouse gas emissions, whilst producing  
7 alternative dispatchable energy (Shen et al., 2015). The biogas industry developed rapidly in  
8 Europe, in particular in Germany with 62% of the total biogas plants (Torrijos, 2016). Biogas  
9 satisfied 4.7% of electricity and 1% of heat demand in Germany in 2014 (Torrijos, 2016). Due to  
10 the high growth rate and carbohydrate content, algae including micro- and macro-algae are  
11 considered to be a viable alternative energy feedstock that is devoid of the major drawbacks  
12 associated with first and second-generation feedstock (Chen et al., 2015; Nigam & Singh, 2011).  
13 However, AD of algae involving biological, chemical, and physical reactions can be limited by the  
14 long retention time, low biodegradation efficiency, and low biogas production rate. The energy  
15 conversion efficiency and process stability of AD can be easily disturbed by various biological and  
16 environmental factors, such as process temperature, pH value, hydrodynamics, and organic  
17 loading and detention time (Cheng & Call, 2016; Viggi et al., 2014).

18 The AD performance needs to be improved to make the process more economically viable.  
19 Optimizations of the process control variables were reported effective to minimize energy  
20 consumption and increase biogas production (Kusiak & Wei, 2012; Wei & Kusiak, 2012). Wei et  
21 al developed a data-driven prediction model to optimize biogas production from sludge, in which  
22 temperature, total solids, volatile solids and pH were employed as controllable variables. A 20.8%

1 increase was obtained when all controllable values were set to the optimal values (Wei & Kusiak,  
2 2012). Many studies have focused on pretreatment development (such as thermal, mechanical,  
3 chemical and biological methods) to overcome feedstock recalcitrance and enhance subsequent  
4 AD performance (Ariunbaatar et al., 2014). The effects of various pretreatment methods are  
5 highly different depending on the feedstock characteristics. Nevertheless, pretreatment methods  
6 could be unsustainable in terms of environmental impacts, even if they enhance AD efficiency  
7 (Ariunbaatar et al., 2014; Carballa et al., 2011).

8 From a biological perspective, AD is carried out by different groups of microorganisms  
9 involved in hydrolysis, acidogenesis, acetogenesis and methanogenesis; interspecies electron  
10 transfer between syntrophic bacteria and methanogenic archaea plays a vital role in enhancing AD  
11 efficiency (Stams & Plugge, 2009). The predominant understanding for interspecies electron  
12 transfer in AD was based on mediated interspecies electron transfer (MIET) via hydrogen or  
13 formate (Rotaru et al., 2014b; Storck et al., 2016). MIET is normally endergonic under standard  
14 conditions and is feasible only at very low metabolite concentration (especially hydrogen) due to  
15 the thermodynamic constraints (Viggi et al., 2014). Recent findings revealed that direct  
16 interspecies electron transfer (DIET) via electrically conductive pili, mineral, or shuttle molecules  
17 is energetically more advantageous than MIET, because DIET does not require the multiple  
18 enzymatic steps to produce hydrogen as an electron carrier (Lovley, 2011; Zhao et al., 2015).

19 Conductive materials (such as nano-magnetite, graphite, biochar, activated carbon and carbon  
20 cloth) may avoid the energy consumption associated with the production of extracellular  
21 conductive pili and associated c-type cytochromes for the provision of biological electrical  
22 connections between cells (Kato et al., 2012; Liu et al., 2012; Zhao et al., 2015). Activated carbon

1 has been proven to promote DIET in AD of different types of substrates, such as ethanol,  
2 propionate, butyrate and glucose (Lee et al., 2016; Zhao et al., 2016b). The biomethane production  
3 rate in the presence of biochar increased by 16-25% in AD of propionate and butyrate (Zhao et al.,  
4 2016a). Carbon-based nanomaterials exhibited the potential to stimulate DIET using glucose and  
5 sucrose as substrates (Li et al., 2015; Tian et al., 2017). Tian et al. demonstrated that  
6 methanogenesis of glucose was improved by addition of graphene during long-term anaerobic  
7 digestion under low temperature (10-20 °C). Despite the establishment of DIET in pure and mixed  
8 cultures, the application of nano-scale carbonaceous materials in traditional AD requires further  
9 investigations to improve the AD performance.

10 As a highly-conductive nanomaterial, graphene has received heightened attention for  
11 biotechnological applications, such as electrode materials in microbial fuel cells (ElMekawy et al.,  
12 2016; Perreault et al., 2015). Graphene has known antimicrobial properties in some cases  
13 (Catherine et al., 2012; Nguyen et al., 2017), however, little is known about the impact of  
14 graphene on anaerobic microbial communities in AD. The unique physicochemical properties of  
15 graphene, notably its exceptionally high electric conductivity, large surface area and good  
16 mechanical strength, may provide a solution to improve the stability and efficiency of AD.  
17 Therefore, it is hypothesized that graphene can significantly facilitate DIET and enhance AD  
18 efficiency. However, to the best of our knowledge, the research of DIET in AD of ethanol in the  
19 presence of graphene is rather sparse. Theoretical comparison of electron transfer flux between  
20 graphene-based DIET and MIET have not been calculated previously. The interactions between  
21 nanomaterial and microbes in AD have not been revealed. In this study, ethanol was used as  
22 feedstock to investigate DIET in AD, as ethanol is a key intermediate product after acidogenesis of

1 algae feedstock (accounting for 15.6%-34.2% of total energy production (Xia et al., 2015; Xia et  
2 al., 2016)). The innovation and objectives of this study are as follows: (1) Compare the kinetics of  
3 biomethane production with different additions of graphene and activated charcoal in AD of  
4 ethanol; (2) Identify the bacterial and archaeal communities responsible for graphene-based DIET  
5 in AD; (3) Calculate the maximum electron transfer flux of MIET and graphene-based DIET for  
6 the first time.

7

## 8 **2. Materials and methods**

### 9 **2.1. Inoculum and materials**

10 The inoculum was sourced from a laboratory digester mainly treating cellulose. Graphene and  
11 activated charcoal were both purchased from Shanghai Aladdin Bio-Chem Technology Co., Ltd,  
12 China. The size of activated charcoal was approximately 10-32 mesh (equivalent to 0.5-1.7 mm).  
13 The micro size of graphene was around 5~10  $\mu\text{m}$ , and the thickness of graphene nanoplatelets was  
14 between 4-20 nm. More details on physic-chemical properties of graphene are available in  
15 [http://www.aladdin-e.com/up\\_files/docs/G139804.pdf](http://www.aladdin-e.com/up_files/docs/G139804.pdf).

16

### 17 **2.2. Experimental design**

18 Batch experiments of AD were conducted in glass fermenters (300 mL working volume). Each  
19 bottle contained 2.5 mL of ethanol as feedstock and 250 mL of activated sludge as inoculum. The  
20 initial pH was adjusted to  $7.5 \pm 0.1$  through use of 6 M HCl and 6 M NaOH solution.

21 Subsequently different amounts of graphene and activated charcoal were separately added into the  
22 glass bottles. The concentrations of graphene were set as 0, 0.5, 1.0 and 2.0 g/L. Considering the

1 electric conductivity of activated charcoal is much lower than that of graphene, the concentrations  
2 of activated charcoal were set as 0, 5, 10, 20 and 30 g/L. Deionized water was added to adjust the  
3 total solution to 300 mL. Afterwards, all the bottles were sealed with rubber stoppers, purged with  
4 nitrogen gas for 10 min, and maintained at  $35 \pm 1.0$  °C during AD. The produced biogas and liquid  
5 solution during methanogenesis were sampled and analyzed at an interval of 2 d. The pH value of  
6 solutions was readjusted to 7.5 every 2 d in order to prevent a severe pH drop during AD. All the  
7 experiments were conducted in duplicate.

8

### 9 **2.3. Microbial community analysis**

10 A volume of 5ml of anaerobic sludge was collected from the bottom of the reactors after the AD  
11 experiments. The sludge samples were rinsed with phosphate-buffered saline and then centrifuged  
12 for 10 min at 4 °C. The pretreated samples were stored at -20 °C until further use. The microbial  
13 community was characterized using high-throughput 16S rRNA pyrosequencing. DNA extraction  
14 was performed following the manufacturer's protocol  
15 ([http://omegabiotek.com/store/wp-content/uploads/2013/04/D5625-Soil-DNA-Kit-101216-online-](http://omegabiotek.com/store/wp-content/uploads/2013/04/D5625-Soil-DNA-Kit-101216-online-1.pdf)  
16 [1.pdf](http://omegabiotek.com/store/wp-content/uploads/2013/04/D5625-Soil-DNA-Kit-101216-online-1.pdf)). The DNA samples were amplified in two independent PCR reactions with primers  
17 spanning the V3-V4 hypervariable region of the 16S rRNA gene. PCR products were checked in 2%  
18 agarose gel to determine the success of amplification. Samples were pooled together in equal  
19 proportions based on their molecular weight and DNA concentrations. Then the samples were  
20 purified using calibrated Ampure XP beads. The pooled and purified PCR product was used to  
21 prepare the DNA library by following Illumina TruSeq DNA library preparation protocol.  
22 Sequencing was performed at MR DNA ([www.mrdnalab.com](http://www.mrdnalab.com), Shallowater, TX, USA) on a MiSeq



1 following the manufacturer's guidelines. Sequence data were processed using MR DNA analysis  
2 pipeline (MR DNA, Shallowater, TX, USA). Operational taxonomic units (OTUs) were defined  
3 by clustering at 3% divergence (97% similarity). Final OTUs were taxonomically classified using  
4 BLASTN against a curated database derived from GreenGenes, RDP II and NCBI  
5 ([www.ncbi.nlm.nih.gov](http://www.ncbi.nlm.nih.gov), <http://rdp.cme.msu.edu>) (DeSantis et al., 2006).

6

#### 7 **2.4. Microscope observation**

8 The microbial morphology of sludge in response to graphene was observed on a field emission  
9 scanning electronic microscope (SEM, Hitachi SU 8010, Japan) (Cheng et al., 2013). The samples  
10 from the reactors were fixed with 2.5% (v/v) glutaraldehyde at 4 °C, washed followed by stepwise  
11 dehydration in a gradient series of ethanol solutions and then CO<sub>2</sub> critical point dried. Samples  
12 were finally coated with gold and observed by SEM.

13

#### 14 **2.5. Analytical methods**

15 The concentrations of biomethane and carbon dioxide were analyzed on a gas chromatography  
16 system (GC; Agilent 7820A, USA) equipped with a thermal conductivity detector and a 5A  
17 column. The concentrations of ethanol and acetate were analyzed on another GC system equipped  
18 with a flame ionization detector and a DB-FFAP column (Lin et al., 2016).

19 Biomethane yield was simulated by the modified Gompertz equation (Eq. 1), and kinetic  
20 parameters ( $H_m$ , maximum methane yield potential, mL/g ethanol;  $R_m$ , peak methane production  
21 rate, mL/g ethanol/h;  $\lambda$ , lag-phase time of methane production, h; and  $T_m$ , peak time of methane  
22 fermentation, h) were calculated using Origin 8.5 software.

$$H = H_m \exp \left\{ -\exp \left[ \frac{R_m e}{H_m} (\lambda - t) + 1 \right] \right\} \quad (1)$$

The degradation of ethanol was assumed to fit a first-order model (Eq. 2), where  $C_e$  is ethanol concentration (mM),  $C_{e0}$  is the initial ethanol concentration (mM), and  $k_e$  is the ethanol degradation rate constant ( $d^{-1}$ ).

$$C_e = C_{e0} \exp(-k_e t) \quad (2)$$

The overall electron recovery after AD of ethanol was calculated according to Eq. 3.

$$\text{Electron recovery \%} = \frac{\text{Actual biomethane yield}}{\text{Stoichiometric conversion of ethanol to biomethane}} \times 100\% \quad (3)$$

8

### 9 **3. Results and discussion**

#### 10 **3.1 Effects of conductive materials on biomethane production kinetics in**

#### 11 **anaerobic digestion**

12 To evaluate the effects of the conductive materials (graphene and activated charcoal) on the  
 13 performance of AD, ethanol (a low-molecular substrate) was used as a model carbon source. The  
 14 effects of graphene and activated charcoal on biomethane yield and production rate are shown in  
 15 Fig. 1 a and b. The biomethane yield from ethanol without conductive material addition was  
 16  $556.1 \pm 53.3$  mL/g after 12 d. The peak biomethane production rate was obtained as  $80.1 \pm 0.2$   
 17 mL/g/d at 4 d. The addition of 20.0 g/L of activated charcoal gave a maximum biomethane yield  
 18 of  $627.2 \pm 30.7$  mL/g. The peak biomethane production rate was obtained as  $91.1 \pm 18.6$  mL/g/d.

19 The biomethane yield and peak biomethane production rate were greatly enhanced by 12.8% and  
 20 13.7%, respectively. The biomethane yields achieved with 5.0, 10.0 and 30.0 g/L of activated

21 charcoal were lower than that with 20.0 g/L of activated charcoal (data were not shown in Fig. 1 in  
 22 order to make it more explicit). Therefore, the optimal concentration of 20.0 g/L activated

1 charcoal was used for further comparison with different concentrations of graphene. It was proven  
2 that carbonaceous materials such as graphite, biochar, and carbon cloth are capable of promoting  
3 methane fermentation and chemical oxygen demand removal (Zhao et al., 2015). Li et al. reported  
4 that the electrical conductance of the sludge was enhanced in the presence of carbon nanotube,  
5 which might promote DIET among fermentative bacteria and methanogens in the AD process (Li  
6 et al., 2015). Thus, it is hypothesized that materials with higher conductivity may play a more  
7 significant role in promoting DIET. Fig. 1 shows that the biomethane yield positively increased  
8 from  $556.1 \pm 53.3$  (0 g/L graphene) to  $670.9 \pm 16.0$  (0.5 g/L graphene),  $695.0 \pm 9.1$  (1.0 g/L graphene)  
9 and  $662.9 \pm 14.7$  mL/g (2.0 g/L graphene). The optimal concentration of graphene (1.0 g/L)  
10 resulted in a 25.0% increase in biomethane yield and a 19.5% increase in peak biomethane  
11 production rate. However, on further increasing the graphene concentration to 2.0 g/L, the  
12 biomethane yield slightly decreased to  $662.9 \pm 14.7$  mL/g. This result was probably ascribed to the  
13 microbial inhibition effect by the high concentration of graphene, indicating that cytotoxicity  
14 could become a limiting factor when applying nanomaterials in AD. Cytotoxicity of carbon  
15 nanomaterials (such as graphene and carbon nanotube) to microbes has been demonstrated using  
16 different microbial strains such as *Escherichia coli* and *Bacillus subtilis* (Liu et al., 2011; Pasquini  
17 et al., 2012; Zhu et al., 2014). The toxicological molecular mechanisms of nanomaterials remained  
18 limited, but a possible explanation was related to the synergistic impacts of cell membrane  
19 perturbation and oxidative stress (Qu et al., 2015).

20 It was noted that the optimal graphene addition resulted in a more significant enhancement of  
21 biomethane production as compared to the optimal activated charcoal addition (even with a  
22 concentration of 20.0 g/L). This result can be ascribed to the following reasons: (1) The electrical

1 conductivity of graphene is much higher than that of activated charcoal, resulting in higher  
2 electron transfer efficiency in DIET; (2) The micro size of graphene is much smaller, resulting in a  
3 higher specific surface area and a better interaction with microbes.

4 The kinetic parameters of biomethane production fitted by the modified Gompertz equation  
5 are shown in Table 1. The kinetics of biomethane production were evaluated in terms of the  
6 biomethane yield potential ( $H_m$ ), peak biomethane production rate ( $R_m$ ), lag phase time ( $\lambda$ ) and  
7 peak time ( $T_m$ ). The maximum biomethane yield potential ( $H_m$ , 718.4 mL/g) was achieved in the  
8 presence of 1.0 g/L graphene, corresponding to a value of 23.4% higher than the control.  
9 Accordingly, the peak biomethane production rate ( $R_m$ , 116.2 mL/g/h) was obtained with the  
10 addition of 1.0 g/L graphene, corresponding to a value of 33.7% higher than the control. The lag  
11 phase time ( $\lambda$ ) and peak time ( $T_m$ ) both reduced to a great extent in the presence of graphene. On  
12 comparison to graphene, the biomethane production performance in terms of biomethane yield  
13 potential and peak biomethane production rate was less enhanced with addition of activated  
14 charcoal, even at a high concentration of 20.0 g/L.

### 16 **3.2 Effects of conductive materials on ethanol degradation in anaerobic digestion**

17 The complete conversion of ethanol to biomethane in AD requires the combined acetogenic  
18 bacteria and methanogenic archaea mediating the three step reactions (Table 2). Acetogenic  
19 bacteria are responsible for converting ethanol into acetate and releasing electrons. Methanogenic  
20 archaea are responsible for converting produced acetate, carbon dioxide and electron into  
21 biomethane. The effects of graphene and activated charcoal on degradation of ethanol are shown  
22 in Fig. 2a. It was observed that ethanol was continuously consumed by acetogenic bacteria during

1 12 d of AD. Ethanol degradation was more rapid with the addition of conductive materials. In the  
2 presence of 1.0 g/L graphene and 20.0 g/L activated charcoal, 50.3% and 43.5% of ethanol were  
3 consumed in the first 2d of AD. Comparatively, only 32.0% of ethanol was consumed in the  
4 absence of conductive materials. Apparently, graphene played a significant role in rapid  
5 degradation of ethanol, which is possibly due to the high electrical conductivity and specific  
6 surface area. The ethanol degradation rate constants derived from the first-order equation are  
7 shown in Fig. 2b. In the absence of conductive materials, the calculated ethanol degradation rate  
8 constant was only  $0.31 \pm 0.03$  /d. This value increased to  $0.37 \pm 0.04$  /d and  $0.40 \pm 0.03$  /d with the  
9 addition of activated charcoal and graphene, respectively. The higher ethanol degradation rate  
10 constant indicated that the substrate degradation in AD can be significantly enhanced through the  
11 presence of conductive materials.

12 With continuous degradation of ethanol, acetate reached a peak concentration, and was  
13 subsequently depleted by aceticlastic methanogen (Fig. 2c). The highest acetate concentration of  
14 58.1 mM was obtained at 6 d in the presence of 1.0 g/L graphene, as compared to acetate  
15 concentration of 43.4 mM in the absence of conductive materials. Ethanol and acetate were  
16 completely consumed at the end of AD (12 d). It was clearly observed that acetate generation by  
17 acetogenic bacteria and subsequent consumption by aceticlastic methanogens were much faster in  
18 the presence of graphene, resulting in promoted methanogenesis and enhanced biomethane yield.  
19 These result indicated that conductive materials are capable of promoting syntrophic reactions  
20 between acetogenic bacteria and methanogenic archaea, which facilitates substrate degradation  
21 and utilization for enhanced methanogenesis.

22 To evaluate the overall efficiency of ethanol conversion in AD, the electron recovery was

1 calculated in terms of biomethane yield and stoichiometric conversion of ethanol to biomethane  
2 (Fig. 2d). Consistent with the biomethane yield, the highest electron recovery of  $95.1\pm 1.2\%$  was  
3 achieved in the presence of graphene, as compared to  $76.1\pm 7.3\%$  in control group. The enhanced  
4 electron recovery was attributed to enhanced DIET efficiency with graphene. It was noteworthy  
5 that 100% conversion of ethanol to biomethane was almost impossible. This was mainly because  
6 the biodegradation of ethanol in AD not only generates acetate (Table 2) but also minor amounts  
7 of propionate, butyrate, or caproate along with the consumption of hydrogen. In addition, some  
8 energy derived from ethanol degradation is required to support microbial growth.

### 10 **3.3 Microbial community analyses after anaerobic digestion**

#### 11 **3.3.1. Bacterial community composition**

12 The enhanced biomethane production was highly dependent on the syntrophic activities of  
13 electron-producing acetogens and electron-consuming methanogens. The changes in the microbial  
14 community might provide a clue to the reason for enhanced biomethane production. Bacterial and  
15 archaeal community structures at genus level after AD of ethanol are shown in Table 3 and 4. The  
16 taxonomic compositions of the initial inoculum were distinctly different from those fed with  
17 ethanol after AD. This result is ascribed to the assimilation effect as ethanol is the only carbon  
18 source, which selectively enriched strains favoring ethanol utilization.

19 In the original inoculum, *Clostridium* (10.1%), *Levilinea* (7.6%), and *Aminobacterium* (4.0%)  
20 were the three major bacterial genera. *Clostridium* are metabolically versatile (Lee et al., 2007) and  
21 are the predominant strains involved in dark hydrogen fermentation converting carbohydrates to  
22 hydrogen along with the production of volatile fatty acids (VFAs, such as acetate and butyrate).

1 *Levilinea* are recognized as an anaerobic fermentative bacterium, which ferment sugars and amino  
2 acids into hydrogen, acetic and lactic acids.(Yamada et al., 2006) *Aminobacterium* are capable of  
3 degrading amino acids to VFAs (Baena et al., 1998).

4 After the AD of ethanol without graphene, the dominant bacterial groups shifted to *Levilinea*  
5 (11.6%), *Clostridium* (8.6%), and *Geobacter* (8.4%). The abundance of amino acid-degrading  
6 *Aminobacterium* decreased to 2.1%, which can be ascribed to the absence of amino acids during  
7 AD. *Geobacter* were enriched from 0.3% (in initial inoculum) to 8.4% with ethanol as substrate. A  
8 variety of *Geobacter* species (such as *G. metallireducens*, *G. pickeringii*, and *G. lovleyi*) has the  
9 ability to utilize ethanol as an electron donor to support their growth metabolism (Lovley et al.,  
10 2011).

11 With the addition of graphene in AD, the dominant bacterial groups shifted to *Geobacter*  
12 (9.9%), *Pseudomonas* (6.9%) and *Levilinea* (6.2%). The abundance of *Geobacter* increased to 9.9%  
13 in the presence of graphene, as compared to 8.4% without graphene. The high electrical  
14 conductivity of graphene may contribute to the shift during AD. Graphene enhances the electron  
15 transfer during ethanol degradation by *Geobacter*, which in turn facilitates the growth of  
16 *Geobacter*. *Geobacter* are well-known iron-respiring bacteria and are distributed widely in  
17 anaerobic environments; they are among the most effective microorganisms for harvesting  
18 electrical current from organic compounds (Lovley et al., 2011). It has been reported that  
19 *Geobacter* play a significant role in performing DIET either directly through extracellular pili or  
20 using additional conductive materials (Cheng & Call, 2016). DIET was first documented in  
21 co-culture of *Geobacter* species, where *Geobacter metallireducens* is capable of transferring  
22 electrons derived from ethanol to the partner *Geobacter sulfurreducens* via electrically conductive

1 pili (Summers et al., 2010). DIET was also recorded in anaerobic digesters where *Geobacter*  
2 transfer electrons to *Methanosaeta* (Rotaru et al., 2014b). DIET may yield more energy than  
3 conventional MIET because there is less energy loss associated with the formation of  
4 intermediates and the subsequent reactions needed to oxidize them (Lovley, 2011; Zhao et al.,  
5 2015). This could be one plausible explanation for the acceleration of methanogenesis in the  
6 presence of graphene. Therefore, it is concluded that the predominance of *Geobacter* population  
7 (9.9%) found in the presence of graphene is a potent support for DIET in AD of ethanol. It was  
8 also found the abundance of *Pseudomonas* was greatly increased to 6.9% in the presence of  
9 graphene, as compared to only 1.9% without graphene. *Pseudomonas* species are recognized as  
10 electrogenic bacteria responsible for converting VFAs to electric current in microbial fuel cells  
11 (Freguia et al., 2010). *Pseudomonas* are also capable of converting ethanol to acetate along with  
12 the production of electrons. However, it was reported that *Pseudomonas* are unable to effectively  
13 transfer electrons derived from central metabolism to the outside of the cell (Lovley, 2006). It was  
14 demonstrated that *Pseudomonas aeruginosa* yielded poorly conductive pili (Reguera et al., 2005),  
15 which cannot be used as conduit for extracellular electron transfer. The addition of graphene in  
16 AD could act as an alternative to conductive pili and an aid in electron transfer from *Pseudomonas*  
17 to the methanogenic partners during AD, contributing to the enhanced growth of *Pseudomonas*. As  
18 a result, since the electrogenic bacteria of *Geobacter* and *Pseudomonas* species were found greatly  
19 enriched with the addition of graphene, they are proposed to be responsible for DIET in AD of  
20 ethanol.

21

### 22 3.3.2. Archaeal community composition



1 The archaeal community structures at genus level with/without graphene addition after AD of  
2 ethanol are shown in Table 4. The majority of archaeal communities were mainly comprised of 4  
3 archaeal genera. In the original inoculum, *Methanosaeta* were the most dominant species  
4 accounting for 86.1% of the total abundance, followed by *Methanolinea* (6.4%),  
5 *Methanobacterium* (2.7%) and *Methanospirillum* (1.1%). *Methanosaeta* are often abundant in  
6 anaerobic digesters and are mainly acetate-consuming methanogens which cleave acetate into CH<sub>4</sub>  
7 and CO<sub>2</sub> (Table 2). *Methanosaeta* are also capable of receiving electrons via DIET for CO<sub>2</sub>  
8 reduction into CH<sub>4</sub> (Rotaru et al., 2014b). *Methanolinea*, *Methanobacterium* and  
9 *Methanospirillum* are conventionally recognized as hydrogen-consuming methanogens, which  
10 convert CO<sub>2</sub> and H<sub>2</sub> into CH<sub>4</sub> (Table 2).

11 After AD of ethanol, the dominant archaeal groups were greatly changed due to the  
12 acclimatization effect by ethanol. With the addition of graphene in AD, the dominant archaeal  
13 groups shifted to *Methanosaeta* (39.8%), *Methanobacterium* (34.9%) and *Methanolinea* (9.8%). It  
14 was noted that the abundance of *Methanosaeta* decreased to 39.8% in the presence of graphene as  
15 compared to 50.1% without graphene, suggesting that the pathway of CH<sub>4</sub> production by acetate  
16 cleavage was weakened. The abundance of *Methanolinea* decreased from 20.2% to 9.8% with the  
17 addition of graphene. Comparatively, *Methanobacterium* became more predominant, increasing  
18 from 24.0% to 34.9%, while *Methanospirillum* were enriched from 2.2% to 7.8%. The shift of  
19 archaeal structures indicated the metabolic pathway was changed in AD in the presence of  
20 graphene. To date, *Methanosarcina* and *Methanosaeta* species are the only methanogens known to  
21 participate in DIET by directly receiving electrons to reduce CO<sub>2</sub> into CH<sub>4</sub> (Rotaru et al., 2014a;  
22 Rotaru et al., 2014b). However, in this study the enrichment of *Methanobacterium* and

1 *Methanospirillum* with the addition of graphene proposes a possibility that they may play an  
2 important role in performing DIET.

3 The communities of bacteria and archaea observed in the presence of graphene provided a  
4 clue for the reason of enhanced biomethane production and also provided a mechanistic  
5 explanation. Taken together, electrogenic bacteria of *Geobacter* and *Pseudomonas* species along  
6 with archaea *Methanobacterium* and *Methanospirillum* may participate in DIET in AD of ethanol,  
7 contributing to the enhanced AD performance.

8

### 9 **3.4 Effects of conductive materials on microbial morphologies after anaerobic** 10 **digestion**

11 Microbial morphologies after AD with/without graphene addition are shown in Fig. S1 in the  
12 Supplementary material. Rod-shaped cells with different lengths of 1-4  $\mu\text{m}$  are predominant in  
13 both samples with/without graphene addition. It appears that cells are attached together (Fig. S1 c  
14 and d), forming microbial aggregates after digestion in the presence of graphene. The direct  
15 contact of cells in aggregates may allow direct electron transfer during AD. It is also observed that  
16 there are extracellular “microbial nanowires” (~50 nm) formed on cell surfaces, exhibiting typical  
17 characteristic of electrogenic bacteria (such as *Geobacter*). However, it is unknown if these  
18 microbial structures are electrically conductive. It was reported that the aggregates in the  
19 anaerobic reactors treating brewery wastes exhibited a high and metal-like conductance (Morita et  
20 al., 2011; Shrestha et al., 2014). The conductive property of aggregates was ascribed to that  
21 *Geobacter* species, which produce electrically conductive pili with a high and metal-like  
22 conductance (Morita et al., 2011).

1

### 2 **3.5 Theoretical analysis of graphene-based direct interspecies electron transfer** 3 **and interspecies hydrogen transfer**

4 Interspecies electron transfer in AD can rely on either DIET (between electron-producing  
5 acetogens and electron-producing methanogens) or MIET with hydrogen as electron carrier. The  
6 simplified electron transfer mechanisms for DIET and MIET are illustrated in Fig. 3. To  
7 quantitatively compare the electron transfer efficiencies of DIET and MIET, the theoretical  
8 maximum electron carrier fluxes were calculated based on Nernst equation and Fick's diffusion  
9 law (Mao et al., 2015; Viggi et al., 2014). The detailed parameters for calculations were provided  
10 in the Supplementary material.

11 The maximum electron flux for the graphene-based DIET was calculated as following.  
12 Assuming that the electrons are released from ethanol degradation through electron-donating  
13 reaction (Table 2,  $\text{CH}_3\text{CH}_2\text{OH} + \text{H}_2\text{O} \rightarrow \text{CH}_3\text{COO}^- + 5\text{H}^+ + 4\text{e}^-$ ,  $\Delta G^{0'} = -149.64$  kJ/mol), then the  
14 electrons are directly transferred to methanogens via graphene. Methanogens reduce  $\text{CO}_2$  to  $\text{CH}_4$   
15 through electron-consuming reaction (Table 2,  $4\text{H}^+ + 4\text{e}^- + 1/2\text{CO}_2 \rightarrow 1/2\text{CH}_4 + \text{H}_2\text{O}$ ,  $\Delta G^{0'} = 93.98$   
16 kJ/mol). The maximum driving force for electron transfer is given by the redox potential ( $\Delta E$ ) of  
17 the overall reaction ( $\text{CH}_3\text{CH}_2\text{OH} + 1/2\text{CO}_2 \rightarrow 1/2\text{CH}_4 + \text{CH}_3\text{COO}^- + \text{H}^+$ ,  $\Delta G^{0'} = -55.67$  kJ/mol),  
18 which was calculated as 0.136 V. The resulting maximum electron flux via graphene was  
19 determined as approximately  $7 \times 10^{-4}$  A (see calculations in Fig. S2 in the Supplementary  
20 material).

21 To estimate the maximum  $\text{H}_2$  flux in MIET, the concentrations of reactants and products were  
22 set identical to those in DIET. Fick's law is used to compute the rate of  $\text{H}_2$  diffusion from the

1 acetogen to the methanogen (Mao et al., 2015). The maximum driving force for H<sub>2</sub> diffusion  
2 depends on the highest H<sub>2</sub> concentration generated by acetogens and the lowest H<sub>2</sub> concentration  
3 reached by methanogens. The highest H<sub>2</sub> concentration was calculated in terms of the  
4 electron-donating reaction (Table 2, CH<sub>3</sub>CH<sub>2</sub>OH + H<sub>2</sub>O → CH<sub>3</sub>COO<sup>-</sup> + H<sup>+</sup> + 2H<sub>2</sub>, corresponding  
5 to ΔG' = 0), and the lowest H<sub>2</sub> concentration was calculated in terms of the electron-consuming  
6 reaction (Table 2, 2H<sub>2</sub> + 1/2CO<sub>2</sub> → 1/2CH<sub>4</sub> + H<sub>2</sub>O, corresponding to ΔG' = 0). The obtained  
7 highest and lowest H<sub>2</sub> concentrations were approximately 70.8 μM and 1.5 nM, respectively.  
8 Therefore, a maximum H<sub>2</sub> flux was achieved as approximately 3.6 × 10<sup>-6</sup> nmol/s, theoretically  
9 corresponding to an equivalent electric current of 7 × 10<sup>-10</sup> A (see calculations in Fig. S3 in the  
10 Supplementary material).

11 Clearly there is a huge difference in maximum electron transfer rate between graphene-based  
12 DIET and MIET via hydrogen. The maximum electron flux calculated in DIET is theoretically  
13 around 10<sup>6</sup> times higher than that obtained in MIET. The calculations also give a clue that  
14 activated charcoal may not be effective to conduct DIET due to its poor electrical conductivity (~5  
15 orders of magnitude lower than graphene (Adinaveen et al., 2016). It should be pointed out that  
16 several assumptions were made to calculate the electron fluxes, such as the microbial cell shape,  
17 average distance between cells, graphene shape, no energy loss as heat during electron transfer,  
18 and no energy consumption for microbial growth. The driving force for electron transfer is  
19 assumed to be totally determined by Gibbs free energy (ΔG' = 0), which does not consider the  
20 energy conserved for microorganism growth and energy loss as heat during electron transfer.  
21 However, a free energy of about -20 to -15 kJ/mol is normally required to support syntrophic  
22 microbial growth (Schink, 1997). These assumptions will undoubtedly result in the inaccuracy on

1 the final calculated value for MIET and DIET, which necessitate a more accurate model  
2 development. However, in spite of these considerations, the computed difference between MIET  
3 and DIET is so large that the kinetic advantage of the DIET via graphene is apparent. The result  
4 provides evidence that graphene-based DIET can intrinsically sustain electric current flux up to 6  
5 orders of magnitude than that of hydrogen-based MIET, allowing for more efficient electron  
6 transfer in syntrophic mechanism in AD of ethanol.

7

## 8 **Conclusions**

9 Highly-conductive graphene was able to stimulate DIET to boost biomethane yield and  
10 production rate from ethanol. The addition of 1.0 g/L graphene resulted in an enhancement of 25.0%  
11 in biomethane yield and 19.5% in production rate. The degradation rate of ethanol was  
12 simultaneously enhanced. Electrogenic bacteria of *Geobacter* and *Pseudomonas* species along  
13 with archaea *Methanobacterium* and *Methanospirillum* might participate in DIET responsible for  
14 enhanced AD performance. Graphene-based DIET intrinsically sustained a much higher electron  
15 transfer flux than conventional hydrogen transfer. Reutilization of conductive materials should be  
16 considered to make DIET-based AD economically viable.

17

## 18 **Acknowledgements**

19 This collaborative Chinese Irish study was supported by the National key research and  
20 development program-China (2016YFE0117900), National Natural Science Foundation-China  
21 (51676171), Zhejiang Provincial Key Research and Development Program-China (2017C04001),  
22 and also funded by Science Foundation Ireland (SFI) through the Centre for Marine and

1 Renewable Energy (MaREI) under Grant No. 12/RC/2302. The work was also co-funded by Gas  
2 Networks Ireland (GNI) through the Gas Innovation Group, and by ERVIA.

3

#### 4 **References**

- 5 [1] Adinaveen, T., Vijaya, J.J., Kennedy, L.J. 2016. Comparative Study of Electrical  
6 Conductivity on Activated Carbons Prepared from Various Cellulose Materials. *Arabian*  
7 *Journal for Science and Engineering*, **41**, 55-65.
- 8 [2] Ariunbaatar, J., Panico, A., Esposito, G., Pirozzi, F., Lens, P.N.L. 2014. Pretreatment  
9 methods to enhance anaerobic digestion of organic solid waste. *Applied Energy*, **123**,  
10 143-156.
- 11 [3] Baena, S., Fardeau, M.L., Labat, M., Ollivier, B., Thomas, P., Garcia, J.L., Patel, B.K.C.  
12 1998. *Aminobacterium colombiense* gen. nov. sp. nov., an Amino Acid-degrading  
13 Anaerobe Isolated from Anaerobic Sludge. *Anaerobe*, **4**, 241-250.
- 14 [4] Carballa, M., Duran, C., Hospido, A. 2011. Should We Pretreat Solid Waste Prior to  
15 Anaerobic Digestion? An Assessment of Its Environmental Cost. *Environmental Science*  
16 *& Technology*, **45**, 10306-10314.
- 17 [5] Catherine, M.S., Joey, M., Farid, A., Alex, L., Rigoberto, C.A., Debora, F.R. 2012.  
18 Graphene nanocomposite for biomedical applications: fabrication, antimicrobial and  
19 cytotoxic investigations. *Nanotechnology*, **23**, 395101.
- 20 [6] Chen, G., Zhao, L., Qi, Y. 2015. Enhancing the productivity of microalgae cultivated in  
21 wastewater toward biofuel production: A critical review. *Applied Energy*, **137**, 282-291.
- 22 [7] Cheng, J., Sun, J., Huang, Y., Feng, J., Zhou, J., Cen, K. 2013. Dynamic microstructures

- 1 and fractal characterization of cell wall disruption for microwave irradiation-assisted lipid  
2 extraction from wet microalgae. *Bioresource Technology*, **150**, 67-72.
- 3 [8] Cheng, Q., Call, D.F. 2016. Hardwiring microbes via direct interspecies electron transfer:  
4 mechanisms and applications. *Environmental Science: Processes & Impacts*, **18**, 968-980.
- 5 [9] DeSantis, T.Z., Hugenholtz, P., Larsen, N., Rojas, M., Brodie, E.L., Keller, K., Huber, T.,  
6 Dalevi, D., Hu, P., Andersen, G.L. 2006. Greengenes, a Chimera-Checked 16S rRNA  
7 Gene Database and Workbench Compatible with ARB. *Applied and Environmental*  
8 *Microbiology*, **72**, 5069-5072.
- 9 [10] ElMekawy, A., Hegab, H.M., Losic, D., Saint, C.P., Pant, D. 2016. Applications of  
10 graphene in microbial fuel cells: The gap between promise and reality. *Renewable and*  
11 *Sustainable Energy Reviews*.
- 12 [11] Freguia, S., Teh, E.H., Boon, N., Leung, K.M., Keller, J., Rabaey, K. 2010. Microbial fuel  
13 cells operating on mixed fatty acids. *Bioresource Technology*, **101**, 1233-1238.
- 14 [12] Kato, S., Hashimoto, K., Watanabe, K. 2012. Methanogenesis facilitated by electric  
15 syntrophy via (semi)conductive iron-oxide minerals. *Environmental Microbiology*, **14**,  
16 1646-1654.
- 17 [13] Kusiak, A., Wei, X. 2012. Optimization of the activated sludge process. *Journal of Energy*  
18 *Engineering*, **139**, 12-17.
- 19 [14] Lee, J.Y., Lee, S.H., Park, H.D. 2016. Enrichment of specific electro-active  
20 microorganisms and enhancement of methane production by adding granular activated  
21 carbon in anaerobic reactors. *Bioresour Technol*, **205**, 205-12.
- 22 [15] Lee, Y.-J., Romanek, C.S., Wiegel, J. 2007. *Clostridium aciditolerans* sp. nov., an

- 1 acid-tolerant spore-forming anaerobic bacterium from constructed wetland sediment.  
2 *International Journal of Systematic and Evolutionary Microbiology*, **57**, 311-315.
- 3 [16] Li, L.L., Tong, Z.H., Fang, C.Y., Chu, J., Yu, H.Q. 2015. Response of anaerobic granular  
4 sludge to single-wall carbon nanotube exposure. *Water Research*, **70**, 1-8.
- 5 [17] Lin, R., Cheng, J., Ding, L., Song, W., Liu, M., Zhou, J., Cen, K. 2016. Enhanced dark  
6 hydrogen fermentation by addition of ferric oxide nanoparticles using *Enterobacter*  
7 *aerogenes*. *Bioresource Technology*, **207**, 213-219.
- 8 [18] Liu, F.H., Rotaru, A.E., Shrestha, P.M., Malvankar, N.S., Nevin, K.P., Lovley, D.R. 2012.  
9 Promoting direct interspecies electron transfer with activated carbon. *Energy &*  
10 *Environmental Science*, **5**, 8982-8989.
- 11 [19] Liu, S., Zeng, T.H., Hofmann, M., Burcombe, E., Wei, J., Jiang, R., Kong, J., Chen, Y.  
12 2011. Antibacterial Activity of Graphite, Graphite Oxide, Graphene Oxide, and Reduced  
13 Graphene Oxide: Membrane and Oxidative Stress. *ACS Nano*, **5**, 6971-6980.
- 14 [20] Lovley, D.R. 2006. Bug juice: harvesting electricity with microorganisms. *Nat Rev*  
15 *Microbiol*, **4**, 497-508.
- 16 [21] Lovley, D.R. 2011. Live wires: direct extracellular electron exchange for bioenergy and  
17 the bioremediation of energy-related contamination. *Energy & Environmental Science*, **4**,  
18 4896-4906.
- 19 [22] Lovley, D.R., Ueki, T., Zhang, T., Malvankar, N.S., Shrestha, P.M., Flanagan, K.A.,  
20 Aklujkar, M., Butler, J.E., Giloteaux, L., Rotaru, A.E., Holmes, D.E., Franks, A.E.,  
21 Orellana, R., Risso, C., Nevin, K.P. 2011. *Geobacter*: the microbe electric's physiology,  
22 ecology, and practical applications. *Adv Microb Physiol*, **59**, 1-100.



- 1 [23] Mao, X., Stenuit, B., Polasko, A., Alvarez-Cohen, L. 2015. Efficient Metabolic Exchange  
2 and Electron Transfer within a Syntrophic Trichloroethene-Degrading Coculture of  
3 *Dehalococcoides mccartyi* 195 and *Syntrophomonas wolfei*. *Applied and Environmental*  
4 *Microbiology*, **81**, 2015-2024.
- 5 [24] Morita, M., Malvankar, N.S., Franks, A.E., Summers, Z.M., Giloteaux, L., Rotaru, A.E.,  
6 Rotaru, C., Lovley, D.R. 2011. Potential for Direct Interspecies Electron Transfer in  
7 Methanogenic Wastewater Digester Aggregates. *mBio*, **2**, e00159-11.
- 8 [25] Nguyen, H.N., Castro-Wallace, S.L., Rodrigues, D.F. 2017. Acute toxicity of graphene  
9 nanoplatelets on biological wastewater treatment process. *Environmental Science: Nano*,  
10 **4**, 160-169.
- 11 [26] Nigam, P.S., Singh, A. 2011. Production of liquid biofuels from renewable resources.  
12 *Progress in Energy and Combustion Science*, **37**, 52-68.
- 13 [27] Pasquini, L.M., Hashmi, S.M., Sommer, T.J., Elimelech, M., Zimmerman, J.B. 2012.  
14 Impact of surface functionalization on bacterial cytotoxicity of single-walled carbon  
15 nanotubes. *Environ. Sci. Technol.*, **46**, 6297.
- 16 [28] Perreault, F., Fonseca de Faria, A., Elimelech, M. 2015. Environmental applications of  
17 graphene-based nanomaterials. *Chem Soc Rev*, **44**, 5861-5896.
- 18 [29] Qu, Y., Ma, Q., Deng, J., Shen, W., Zhang, X., He, Z., Van Nostrand, J.D., Zhou, J., Zhou,  
19 J. 2015. Responses of microbial communities to single-walled carbon nanotubes in  
20 phenol wastewater treatment systems. *Environ Sci Technol*, **49**, 4627-35.
- 21 [30] Reguera, G., McCarthy, K.D., Mehta, T., Nicoll, J.S., Tuominen, M.T., Lovley, D.R. 2005.  
22 Extracellular electron transfer via microbial nanowires. *Nature*, **435**, 1098-101.

- 1 [31] Rotaru, A.E., Shrestha, P.M., Liu, F., Markovaite, B., Chen, S., Nevin, K.P., Lovley, D.R.  
2 2014a. Direct Interspecies Electron Transfer between *Geobacter metallireducens* and  
3 *Methanosarcina barkeri*. *Applied and Environmental Microbiology*, **80**, 4599-4605.
- 4 [32] Rotaru, A.E., Shrestha, P.M., Liu, F.H., Shrestha, M., Shrestha, D., Embree, M., Zengler,  
5 K., Wardman, C., Nevin, K.P., Lovley, D.R. 2014b. A new model for electron flow during  
6 anaerobic digestion: direct interspecies electron transfer to *Methanosaeta* for the reduction  
7 of carbon dioxide to methane. *Energy & Environmental Science*, **7**, 408-415.
- 8 [33] Schink, B. 1997. Energetics of syntrophic cooperation in methanogenic degradation.  
9 *Microbiology and Molecular Biology Reviews*, **61**, 262-280.
- 10 [34] Shen, Y., Linville, J.L., Urgun-Demirtas, M., Schoene, R.P., Snyder, S.W. 2015.  
11 Producing pipeline-quality biomethane via anaerobic digestion of sludge amended with  
12 corn stover biochar with in-situ CO<sub>2</sub> removal. *Applied Energy*, **158**, 300-309.
- 13 [35] Shrestha, P.M., Malvankar, N.S., Werner, J.J., Franks, A.E., Elena-Rotaru, A., Shrestha,  
14 M., Liu, F.H., Nevin, K.P., Angenent, L.T., Lovley, D.R. 2014. Correlation between  
15 microbial community and granule conductivity in anaerobic bioreactors for brewery  
16 wastewater treatment. *Bioresource Technology*, **174**, 306-310.
- 17 [36] Stams, A.J.M., Plugge, C.M. 2009. Electron transfer in syntrophic communities of  
18 anaerobic bacteria and archaea. *Nature Reviews Microbiology*, **7**, 568-577.
- 19 [37] Storck, T., Virdis, B., Batstone, D.J. 2016. Modelling extracellular limitations for  
20 mediated versus direct interspecies electron transfer. *The ISME journal*, **10**, 621-631.
- 21 [38] Summers, Z.M., Fogarty, H.E., Leang, C., Franks, A.E., Malvankar, N.S., Lovley, D.R.  
22 2010. Direct Exchange of Electrons Within Aggregates of an Evolved Syntrophic

- 1 Coculture of Anaerobic Bacteria. *Science*, **330**, 1413-1415.
- 2 [39] Tian, T., Qiao, S., Li, X., Zhang, M., Zhou, J. 2017. Nano-graphene induced positive  
3 effects on methanogenesis in anaerobic digestion. *Bioresource Technology*, **224**, 41-47.
- 4 [40] Torrijos, M. 2016. State of Development of Biogas Production in Europe. *Procedia*  
5 *Environmental Sciences*, **35**, 881-889.
- 6 [41] Viggi, C.C., Rossetti, S., Fazi, S., Paiano, P., Majone, M., Aulenta, F. 2014. Magnetite  
7 Particles Triggering a Faster and More Robust Syntrophic Pathway of Methanogenic  
8 Propionate Degradation. *Environmental Science & Technology*, **48**, 7536-7543.
- 9 [42] Wei, X., Kusiak, A. 2012. Optimization of biogas production process in a wastewater  
10 treatment plant. *IIE Annual Conference. Proceedings*. Institute of Industrial and Systems  
11 Engineers (IISE). pp. 1.
- 12 [43] Xia, A., Jacob, A., Herrmann, C., Tabassum, M.R., Murphy, J.D. 2015. Production of  
13 hydrogen, ethanol and volatile fatty acids from the seaweed carbohydrate mannitol.  
14 *Bioresource Technology*, **193**, 488-497.
- 15 [44] Xia, A., Jacob, A., Tabassum, M.R., Herrmann, C., Murphy, J.D. 2016. Production of  
16 hydrogen, ethanol and volatile fatty acids through co-fermentation of macro- and  
17 micro-algae. *Bioresource Technology*, **205**, 118-125.
- 18 [45] Yamada, T., Sekiguchi, Y., Hanada, S., Imachi, H., Ohashi, A., Harada, H., Kamagata, Y.  
19 2006. *Anaerolinea thermolimosa* sp. nov., *Levilinea saccharolytica* gen. nov., sp. nov. and  
20 *Leptolinea tardivitalis* gen. nov., sp. nov., novel filamentous anaerobes, and description of  
21 the new classes *Anaerolineae* classis nov. and *Caldilineae* classis nov. in the bacterial  
22 phylum Chloroflexi. *International Journal of Systematic and Evolutionary Microbiology*,

1           **56**, 1331-1340.

2   [46]   Zhao, Z., Zhang, Y., Holmes, D.E., Dang, Y., Woodard, T.L., Nevin, K.P., Lovley, D.R.

3           2016a. Potential enhancement of direct interspecies electron transfer for syntrophic

4           metabolism of propionate and butyrate with biochar in up-flow anaerobic sludge blanket

5           reactors. *Bioresour Technol*, **209**, 148-56.

6   [47]   Zhao, Z., Zhang, Y., Yu, Q., Dang, Y., Li, Y., Quan, X. 2016b. Communities stimulated

7           with ethanol to perform direct interspecies electron transfer for syntrophic metabolism of

8           propionate and butyrate. *Water Res*, **102**, 475-84.

9   [48]   Zhao, Z.Q., Zhang, Y.B., Woodard, T.L., Nevin, K.P., Lovley, D.R. 2015. Enhancing

10          syntrophic metabolism in up-flow anaerobic sludge blanket reactors with conductive

11          carbon materials. *Bioresource Technology*, **191**, 140-145.

12   [49]   Zhu, B., Xia, X., Xia, N., Zhang, S., Guo, X. 2014. Modification of fatty acids in

13          membranes of bacteria: implication for an adaptive mechanism to the toxicity of carbon

14          nanotubes. *Environ. Sci. Technol.*, **48**, 4086.

15

1 **List of figures and tables:**

2

3 Fig. 1 Effects of graphene and activated charcoal on biomethane yield and production rate from  
4 ethanol: (a) biomethane yield, (b) biomethane production rate.

5 Fig. 2 Effects of graphene and activated charcoal on ethanol and acetate conversion: (a) ethanol  
6 degradation kinetics, (b) ethanol degradation rate constant, (c) acetate degradation, and (d) overall  
7 electron recovery.

8 Fig. 3 Mechanisms for extracellular cell-to-cell electron transfer in anaerobic digestion: (a)  
9 mediated interspecies electron transfer, (b) direct interspecies electron transfer via graphene.

10

11 Table 1 Effects of graphene and activated charcoal on biomethane production kinetics.

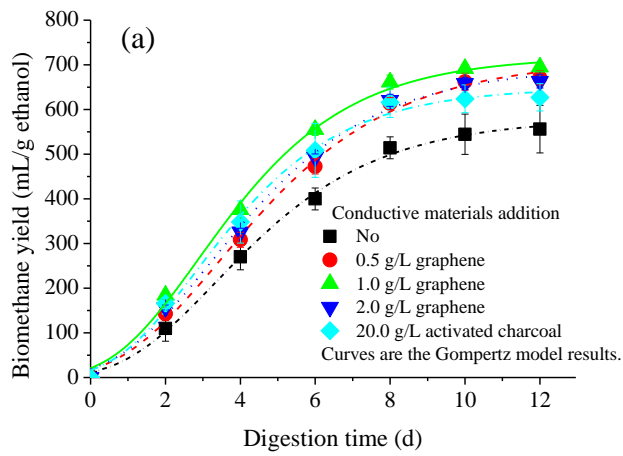
12 Table 2 Three step reactions and thermodynamics in bioconversion of ethanol to biomethane.

13 Table 3 Bacterial community structures at genus level with/without graphene addition after  
14 anaerobic digestion of ethanol. Genera with less than 1% abundances were classified into others.

15 Table 4 Archaeal community structures at genus level with/without graphene addition after  
16 anaerobic digestion of ethanol. Genera with less than 1% abundances were classified into others.

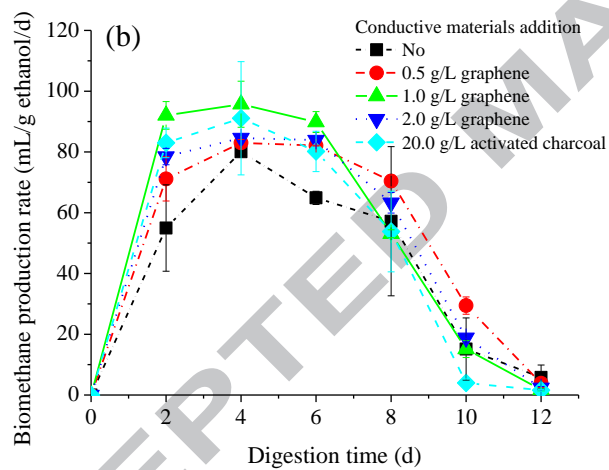
17

1



2

3



4

5 Fig. 1 Effects of graphene and activated charcoal on biomethane yield and production rate from

6 ethanol: (a) biomethane yield, (b) biomethane production rate. Results are the means and standard

7 deviations for duplicate experiments.

8

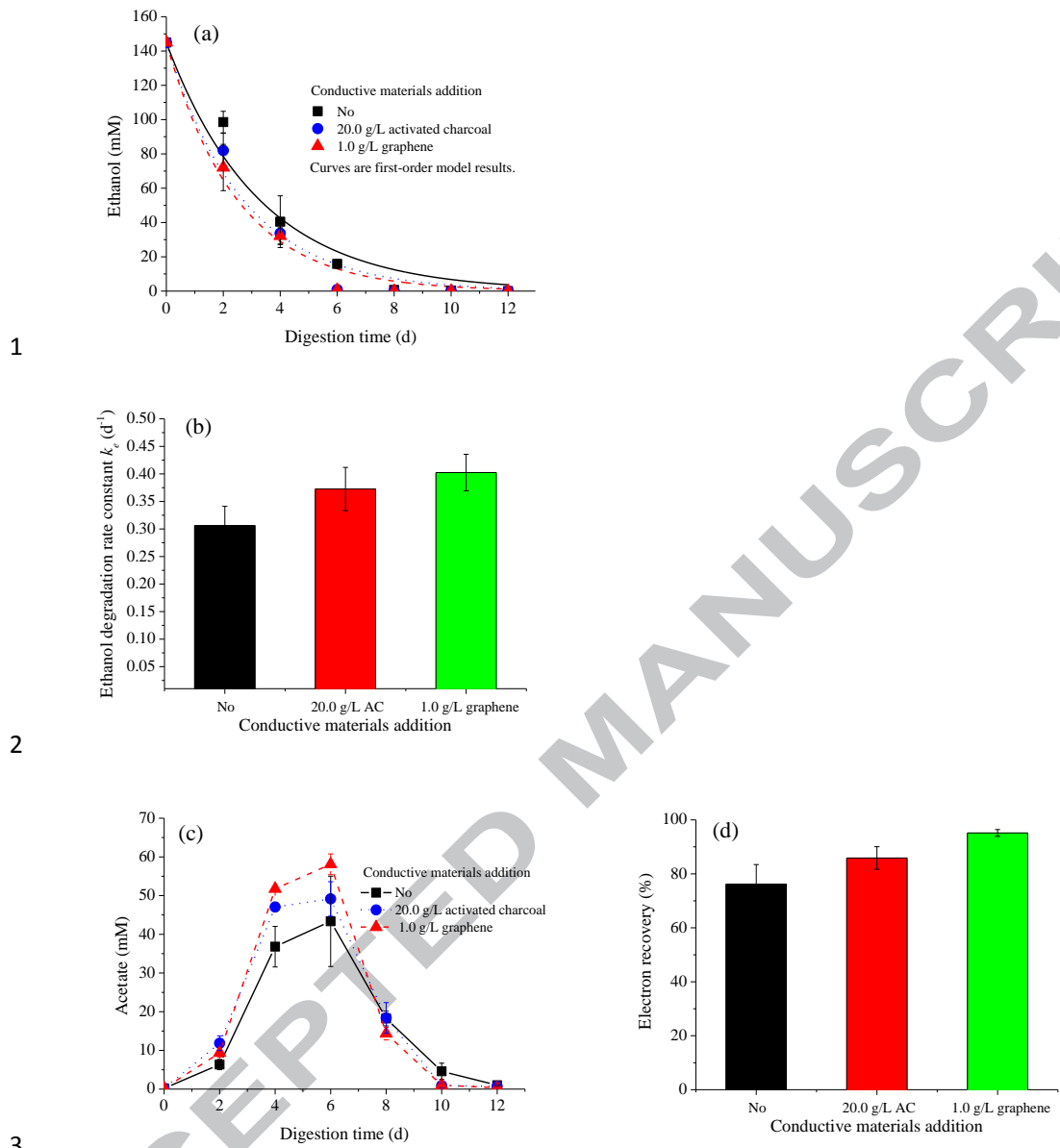
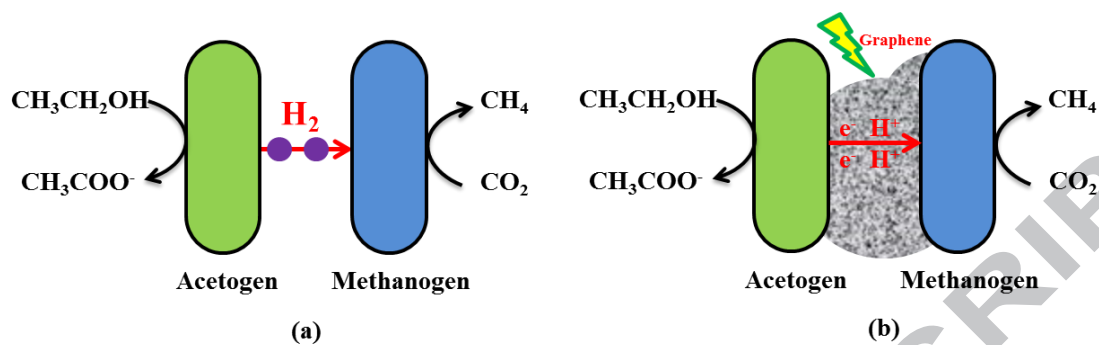


Fig. 2 Effects of graphene and activated charcoal on ethanol and acetate conversion: (a) ethanol degradation kinetics, (b) ethanol degradation rate constant, (c) acetate degradation, and (d) overall electron recovery. Results are the means and standard deviations for duplicate experiments.

1



2

3 Fig. 3 Mechanisms for extracellular cell-to-cell electron transfer in anaerobic digestion: (a)

4 mediated interspecies electron transfer, (b) direct interspecies electron transfer via graphene.

5



6 Table1 Effects of graphene and activated charcoal on biomethane production kinetics.

Conductive materials concentration	Biomethane yield (mL/g)	Peak biomethane production rate (mL/g/d)	Kinetic model parameters				
			$H_m$ (mL/g)	$R_m$ (mL/g/d)	$\lambda$ (d)	$T_m$ (d)	$R^2$
No	556.1±53.3	80.1±0.2	579.7	86.9	0.89	3.34	0.9967
0.5 g/L graphene	670.9±16.0	83.0±1.1	711.2	99.1	0.81	3.45	0.9951
1.0 g/L graphene	695.0±9.1	95.7±7.6	718.4	116.2	0.60	2.87	0.9955
2.0 g/L graphene	662.9±14.7	84.6±1.3	695.7	102.8	0.70	3.19	0.9950
20.0 g/L activated charcoal	627.2±30.7	91.1±18.6	648.8	109.8	0.65	2.82	0.9939

7 Note:  $H_m$ , maximum methane yield potential;  $R_m$ , peak methane production rate;  $\lambda$ , lag-phase time; and  $T_m$ , peak time of methane fermentation.

8 Table 2 Three step reactions and thermodynamics in bioconversion of ethanol to biomethane.

Process	Reactions	$\Delta G_0'^a$ (kJ/mol)
1. Electron-producing acetogen	MIET: $\text{CH}_3\text{CH}_2\text{OH} + \text{H}_2\text{O} \rightarrow \text{CH}_3\text{COO}^- + \text{H}^+ + 2\text{H}_2$	9.68
	DIET: $\text{CH}_3\text{CH}_2\text{OH} + \text{H}_2\text{O} \rightarrow \text{CH}_3\text{COO}^- + 5\text{H}^+ + 4\text{e}^-$	-149.64
2. Electron-consuming methanogen	MIET: $2\text{H}_2 + 1/2\text{CO}_2 \rightarrow 1/2\text{CH}_4 + \text{H}_2\text{O}$	-65.35
	DIET: $4\text{H}^+ + 4\text{e}^- + 1/2\text{CO}_2 \rightarrow 1/2\text{CH}_4 + \text{H}_2\text{O}$	93.98
3. Acetate-consuming methanogen	$\text{CH}_3\text{COO}^- + \text{H}^+ \rightarrow \text{CH}_4 + \text{CO}_2$	-35.91
Overall	$\text{CH}_3\text{CH}_2\text{OH} \rightarrow 3/2\text{CH}_4 + 1/2\text{CO}_2$	-91.58

9 <sup>a</sup>  $\Delta G_0'$  is the free energy change of reaction under standard conditions at pH 7. Negative value indicates the reaction is thermodynamically favorable and proceeds  
10 spontaneously.

11

12 Table 3 Bacterial community structures at genus level with/without graphene addition after anaerobic digestion of ethanol. Genera with less than 1% abundances  
 13 were classified into others.

Genera	Relative abundance in different anaerobic digestates (%)		
	Inoculum	Digestate without graphene	Digestate with 1.0 g/L graphene
<i>Geobacter</i>	0.29	8.43	9.94
<i>Pseudomonas</i>	0.43	1.91	6.85
<i>Levilinea</i>	7.64	11.59	6.2
<i>Clostridium</i>	10.09	8.57	5.15
<i>Thermovirga</i>	3.34	2.71	2.98
<i>Victivallis</i>	0.38	2.89	2.73
<i>Aminobacterium</i>	3.98	2.14	2.24
<i>Longilinea</i>	0.85	2.71	2.22
<i>Desulfovibrio</i>	0.05	2.27	1.96
<i>Synergistes</i>	3.09	1.97	1.72
<i>Smithella</i>	2.86	2.03	1.45
<i>Syntrophomonas</i>	1.4	2.13	1.27
<i>Meniscus</i>	1.86	1.69	1.24
<i>Bellilinea</i>	1.27	1.54	0.9
<i>Others</i>	42.92	34.04	39.39
<i>unclassified</i>	19.55	13.38	13.76

14

15

16 Table 4 Archaeal community structures at genus level with/without graphene addition after anaerobic digestion of ethanol. Genera with less than 1% abundances  
 17 were classified into others.

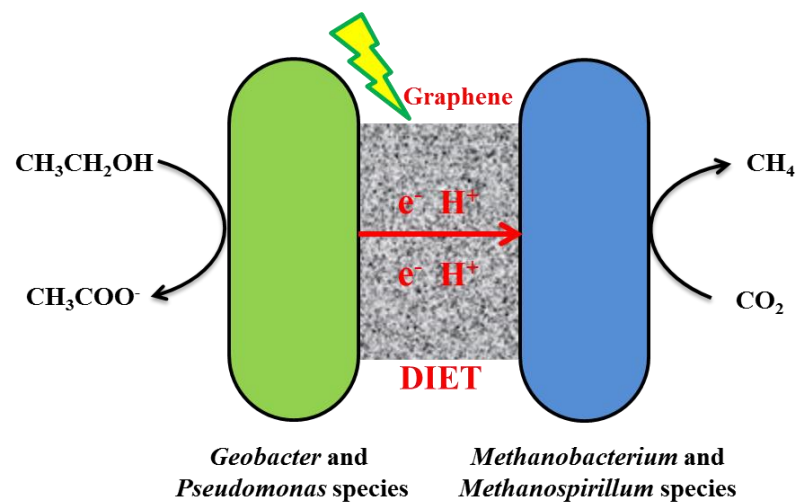
Genera	Relative abundance in different anaerobic digestates (%)		
	Inoculum	Digestate without graphene	Digestate with 1.0 g/L graphene
<i>Methanosaeta</i>	86.08	50.14	39.75
<i>Methanobacterium</i>	2.68	24.02	34.87
<i>Methanolinea</i>	6.44	20.19	9.84
<i>Methanospirillum</i>	1.14	2.15	7.76
unclassified	2.27	2.07	4.66
Others	1.39	1.43	3.12

18

19

## 20 Graphical abstract

21



## 22 Graphene-based DIET in anaerobic digestion

23

23

24 Graphene enhanced methane yield (+25%) and production rate (+20%) in AD of ethanol.

25 Microbial structures of electro-active bacteria and archaea were revealed after AD.

26 Direct interspecies electron transfer (DIET) via graphene was established in AD.

27 DIET sustained much higher electron transfer flux than hydrogen transfer.

28

29